

Kaon SIDIS on proton and deuteron with CLAS12

Simone Vallarino

INFN Genova

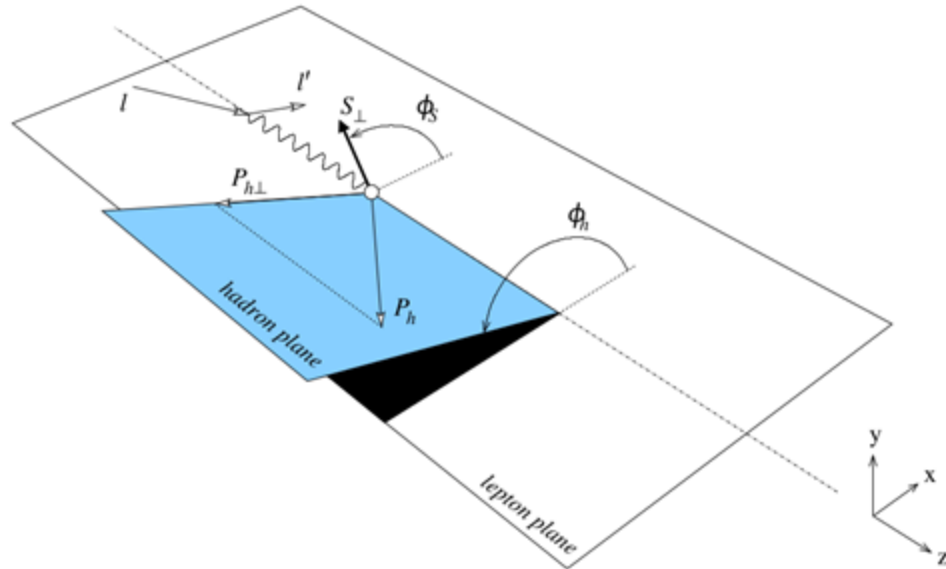
December 15, 2025

Polarized Semi-Inclusive DIS at Jefferson Lab

Polarized Semi-Inclusive DIS

SIDIS is the scattering of a lepton off a nucleon, producing a final state on which the scattered lepton and at least one hadron are detected.

$$\ell(l) + N(P) \rightarrow \ell(l') + h(P_h) + X$$



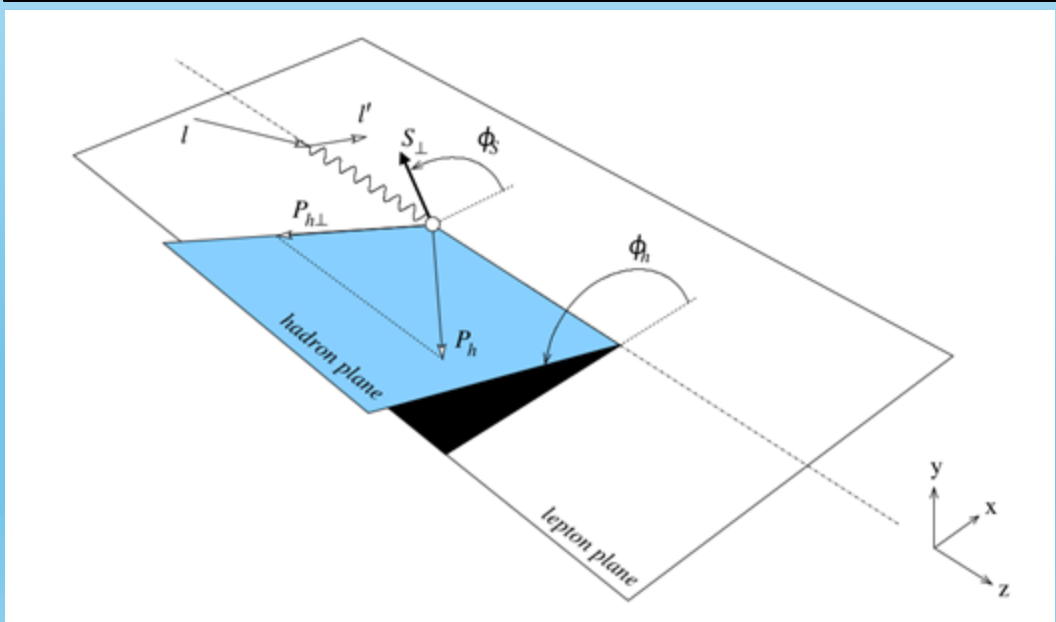
$$\begin{aligned} \frac{d\sigma}{dx dy d\psi dz d\phi_h dP_{h\perp}^2} = & \frac{\alpha^2}{xyQ^2} \frac{y^2}{2(1-\varepsilon)} \left(1 + \frac{\gamma^2}{2x}\right) \left\{ F_{UU,T} + \varepsilon F_{UU,L} + \sqrt{2\varepsilon(1+\varepsilon)} \cos\phi_h F_{UU}^{\cos\phi_h} \right. \\ & + \varepsilon \cos(2\phi_h) F_{UU}^{\cos 2\phi_h} + \lambda_e \sqrt{2\varepsilon(1-\varepsilon)} \sin\phi_h F_{LU}^{\sin\phi_h} \\ & + S_{\parallel} \left[\sqrt{2\varepsilon(1+\varepsilon)} \sin\phi_h F_{UL}^{\sin\phi_h} + \varepsilon \sin(2\phi_h) F_{UL}^{\sin 2\phi_h} \right] \\ & + S_{\parallel} \lambda_e \left[\sqrt{1-\varepsilon^2} F_{LL} + \sqrt{2\varepsilon(1-\varepsilon)} \cos\phi_h F_{LL}^{\cos\phi_h} \right] \\ & + |S_{\perp}| \left[\sin(\phi_h - \phi_S) \left(F_{UT,T}^{\sin(\phi_h - \phi_S)} + \varepsilon F_{UT,L}^{\sin(\phi_h - \phi_S)} \right) \right. \\ & + \varepsilon \sin(\phi_h + \phi_S) F_{UT}^{\sin(\phi_h + \phi_S)} + \varepsilon \sin(3\phi_h - \phi_S) F_{UT}^{\sin(3\phi_h - \phi_S)} \\ & + \sqrt{2\varepsilon(1+\varepsilon)} \sin\phi_S F_{UT}^{\sin\phi_S} + \sqrt{2\varepsilon(1+\varepsilon)} \sin(2\phi_h - \phi_S) F_{UT}^{\sin(2\phi_h - \phi_S)} \left. \right] \\ & + |S_{\perp}| \lambda_e \left[\sqrt{1-\varepsilon^2} \cos(\phi_h - \phi_S) F_{LT}^{\cos(\phi_h - \phi_S)} + \sqrt{2\varepsilon(1-\varepsilon)} \cos\phi_S F_{LT}^{\cos\phi_S} \right. \\ & \left. + \sqrt{2\varepsilon(1-\varepsilon)} \cos(2\phi_h - \phi_S) F_{LT}^{\cos(2\phi_h - \phi_S)} \right] \left. \right\} \end{aligned}$$

Polarized Semi-Inclusive DIS

SIDIS is the scattering of a lepton off a nucleon, producing a final state on which the scattered lepton and at least one hadron are detected.

$$\frac{d\sigma}{dx dy d\psi dz d\phi_h dP_{h\perp}^2} = \frac{\alpha^2}{xyQ^2} \frac{y^2}{2(1-\varepsilon)} \left(1 + \frac{\gamma^2}{2x}\right) \left\{ F_{UU,T} + \varepsilon F_{UU,L} + \sqrt{2\varepsilon(1+\varepsilon)} \cos\phi_h F_{UU}^{\cos\phi_h} \right. \\ \left. + \varepsilon \cos(2\phi_h) F_{UU}^{\cos 2\phi_h} + \lambda_e \sqrt{2\varepsilon(1-\varepsilon)} \sin\phi_h F_{LU}^{\sin\phi_h} \right\}$$

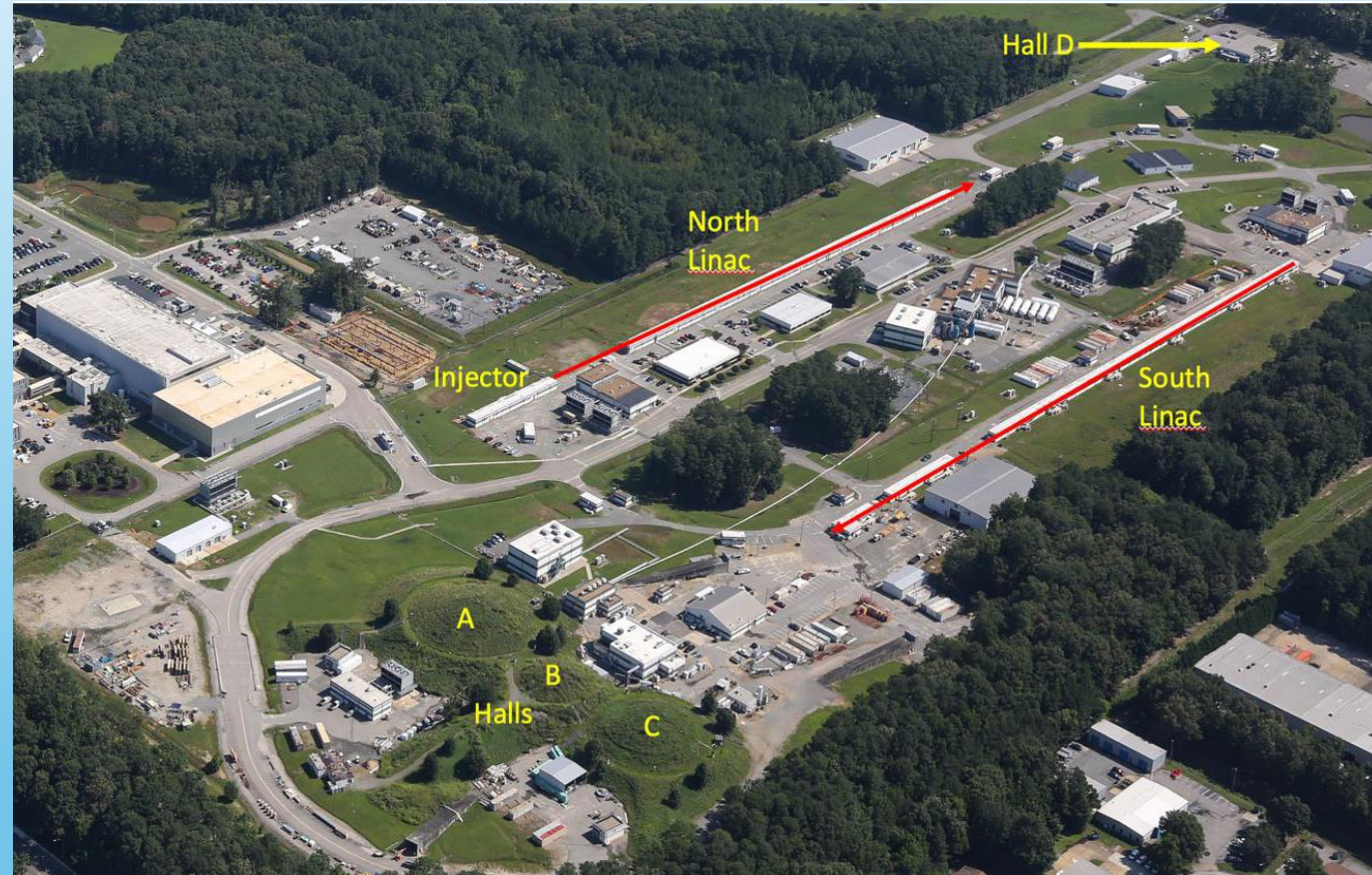
$$\ell(l) + N(P) \rightarrow \ell(l') + h(P_h) + X$$



$$F_{LU}^{\sin\phi} = \frac{2M}{Q} \mathcal{C} \left[\frac{\hat{\mathbf{h}} \cdot \mathbf{k}_T}{M_H} \left(x_B e H_1^\perp + \frac{M_h}{M} f_1 \frac{\tilde{G}^\perp}{z} \right) + \frac{\hat{\mathbf{h}} \cdot \mathbf{p}_T}{M} \left(x_B g^\perp D_1 + \frac{M_h}{M} h_1^\perp \frac{\tilde{E}}{z} \right) \right]$$

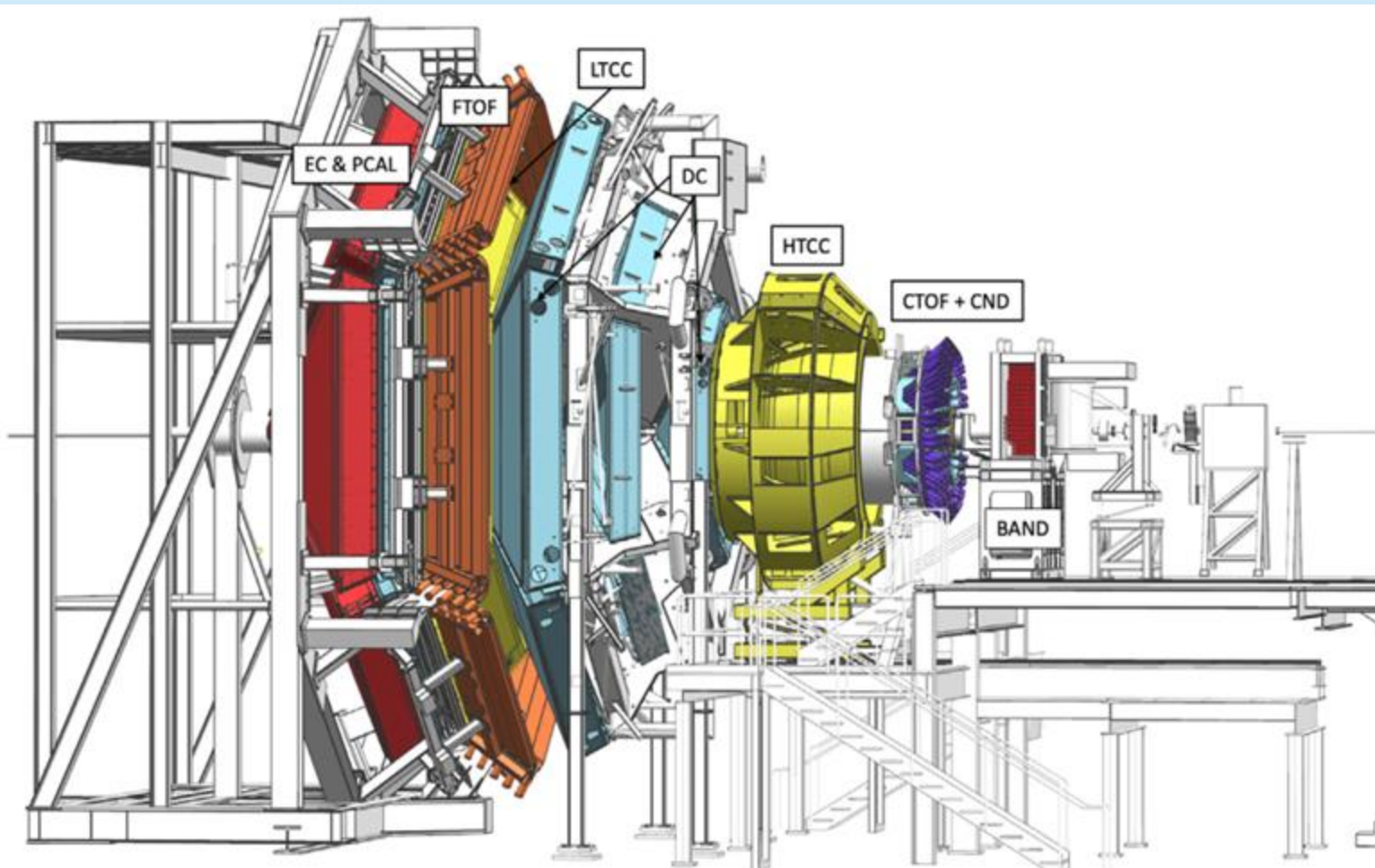
Thomas Jefferson National Accelerator Facility

- National laboratory of the U.S Department of Energy Office of Science;
- JLAB hosts the Continuous Electron Beam Accelerator Facility (CEBAF), a highly intense and highly polarized 12 GeV electron beam;
- Four experimental Halls hosting different apparatuses;
- The goals are to test the standard model and search physics beyond it via:
 - precise parity violation measurements;
 - light dark matter searches;
 - exotic particle searches;
 - three-dimensional nucleon structure;
 - parton dynamics investigation.



The Jefferson Lab at Newport News, VA, USA

CEBAF Large Acceptance Spectrometer for operation at 12 GeV



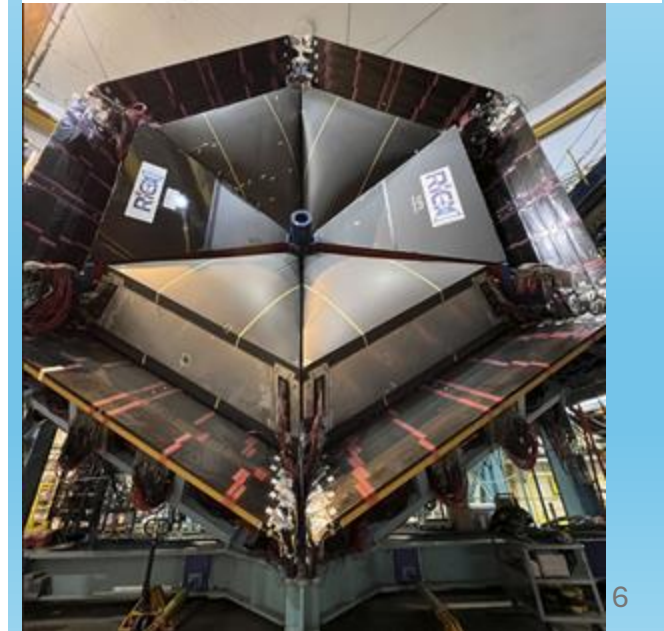
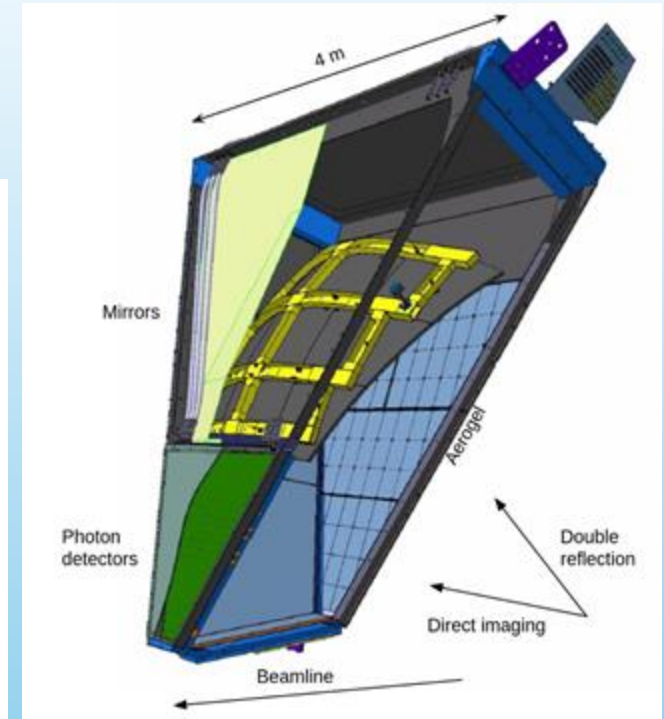
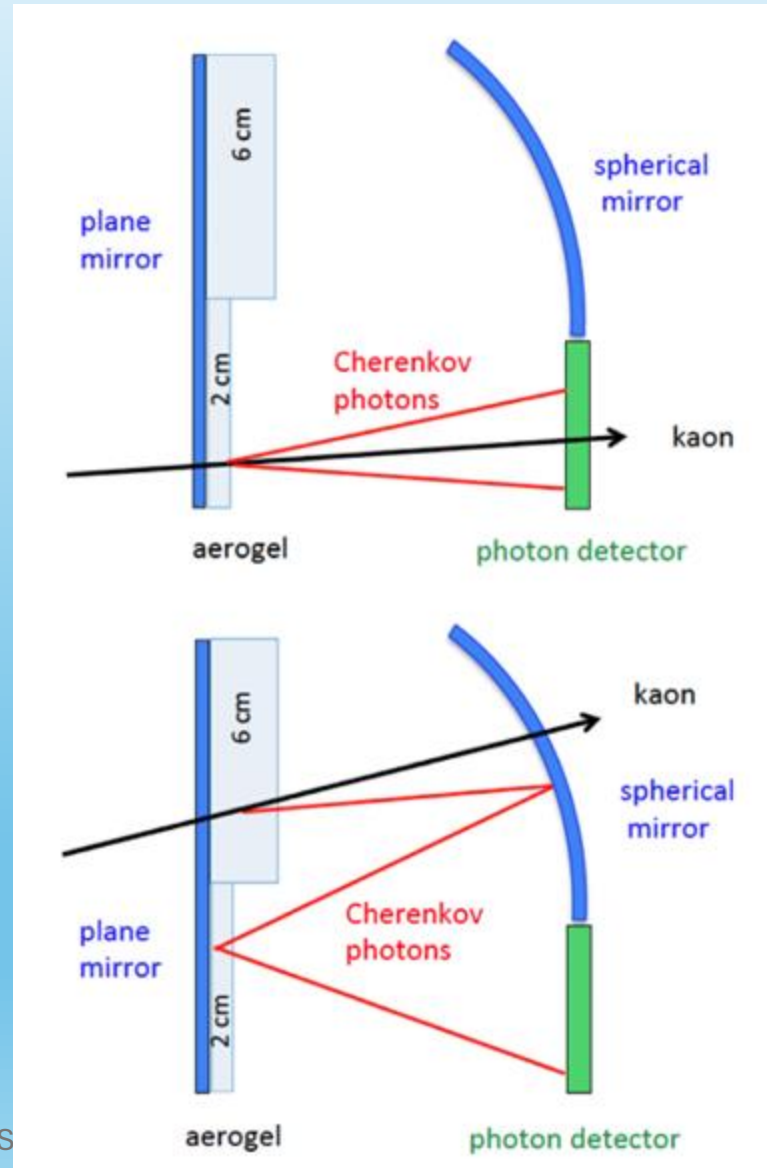
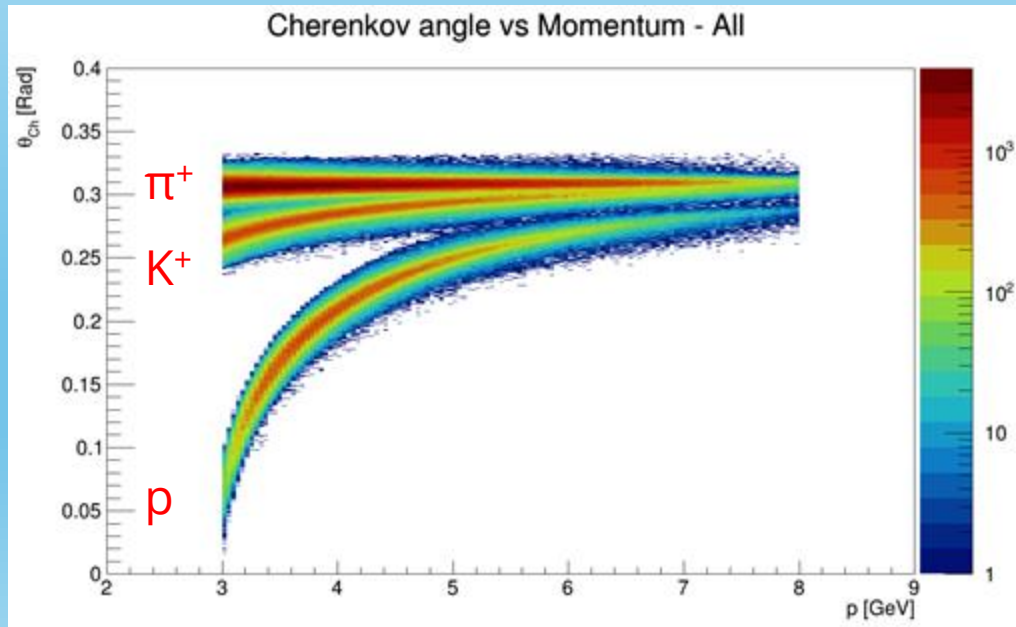
The CLAS12 experiment at CEBAF

- $\mathcal{L} = 10^{35} \text{ cm}^{-2}\text{s}^{-1}$;
- Dual-magnet system;
- Six sectors;
- Almost full azimuthal coverage;
- Forward Detector $5^\circ < \theta < 35^\circ$: drift chambers, Cherenkov counters, time-of-flight, electromagnetic calorimeter;
- Central Detector $35^\circ < \theta < 125^\circ$: vertex tracker, time-of-flight, neutron detector;
- Forward tagger $2.5^\circ < \theta < 4.5^\circ$: electromagnetic calorimeter, micro-strip gas tracker, hodoscope

CLAS12 Ring Imaging Cherenkov

In 2018, one sector was equipped with a RICH detector to improve the π^\pm/K^\pm separation between 3 and 8 GeV/c. The RICH was expected to provide a separation efficiency in order of 99%. In 2022, a second module of RICH was added.

Aerogel refractive index: $n = 1.05$.
Photon detector: Multi-Anode PMT.



High-momentum K^+ SIDIS

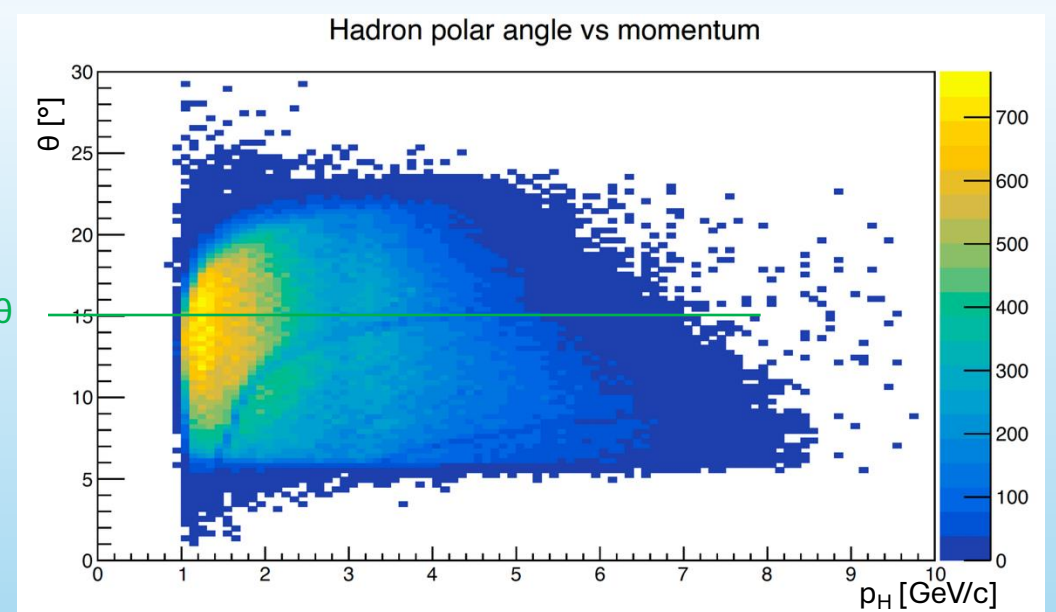
- The study focuses on positive kaon SIDIS, which for the first time in CLAS12 includes high-momentum kaons (> 3 GeV) thanks to the introduction of the RICH, significantly reducing pion contamination.
- The analysis focuses on RG-B data, using RG-A as a reference, allowing the compare scattering off deuteron (RG-B, unpolarized D target) and proton (RG-A, unpolarized H target).
- Particle Identification (PID) plays a crucial role in this analysis.
- In the CLAS12 phase space, the pion yield is approximately four time larger than the kaon yield.
- Even a small inefficiency in PID can lead a large contamination effect.

Analysis status

Analysis status

- RICH alignment:
 - Alignment nearly complete
 - Polar angle coverage extended up to $\sim 23^\circ$
- CLAS12 pass-2 reconstruction:
 - Residual mismatch between RICH geometry, RICH alignment, and global detector alignment;
 - Results in reduced RICH efficiency in pass-2; issue expected to be resolved soon.
- Fiducial cuts:
 - ECAL and DC cuts from RG-A pass-2 [[ref](#)] are currently in use
 - No dedicated RG-B fiducial cuts are available yet
 - RICH fiducial cuts will be updated once the mismatch is fully understood and corrected.

Old limit in θ



Systematic uncertainty

Typical Sources of Systematic Uncertainty in BSA

- Beam polarization → it was evaluated by combining the uncertainty on the measurements of the beam polarization performed during data taking;
- Bin migration → the RICH simulation is available to evaluate the bin migration effect;
- Radiative effects → A. Ilyichev [[1](#), [2](#)] agreed to run the software to estimate the related uncertainty.

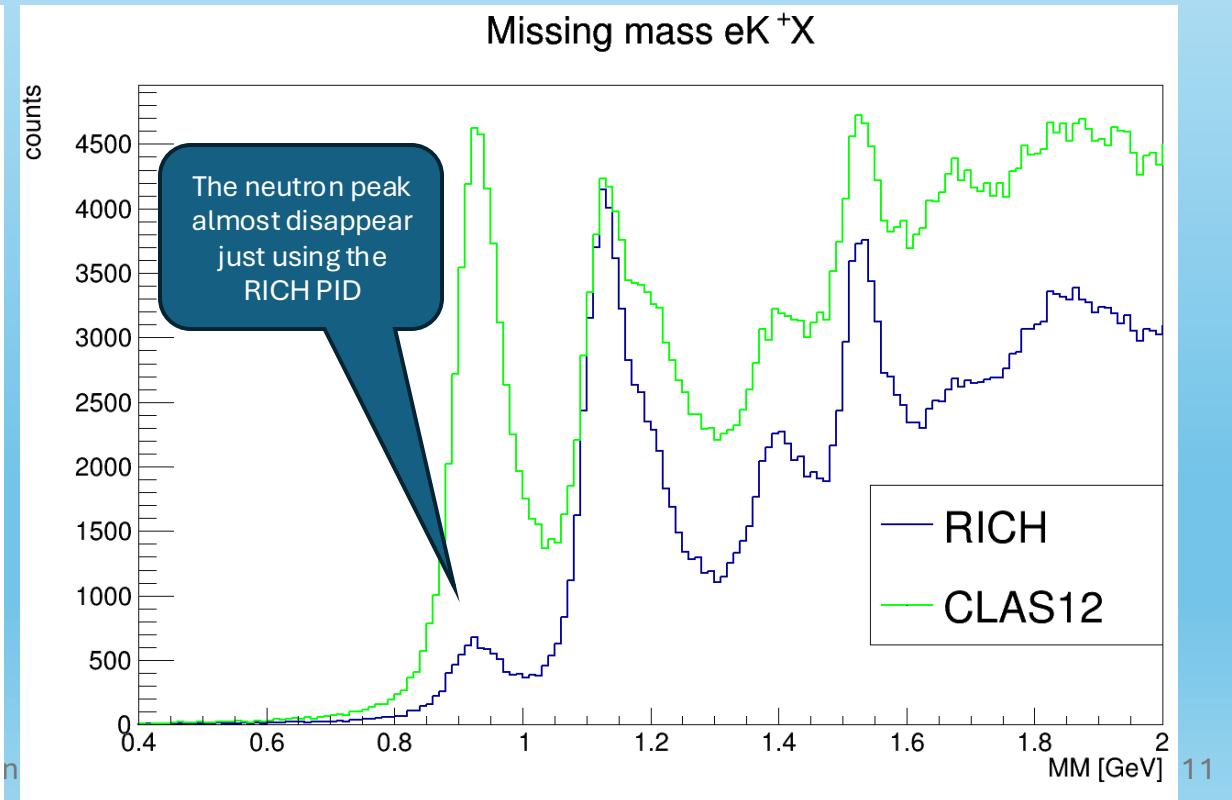
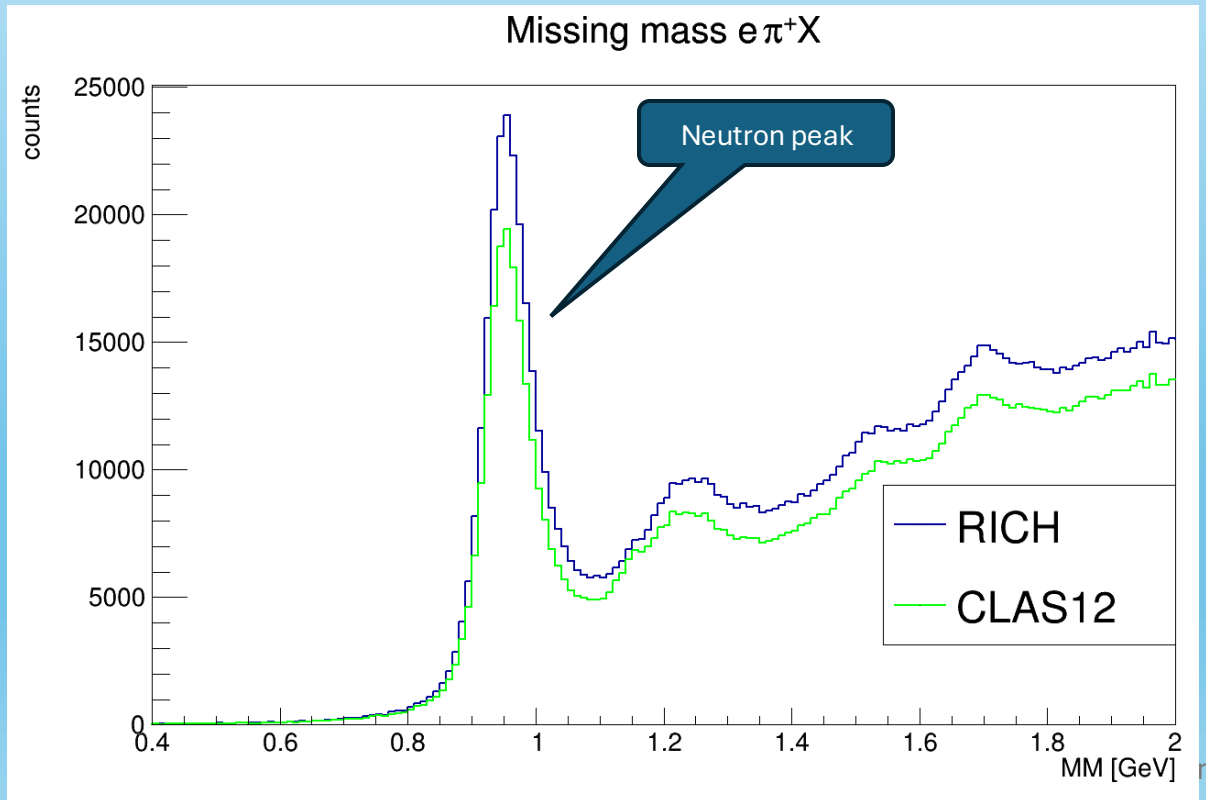
Analysis-Specific Sources

- Pion contamination in the kaon sample → the RICH was added to CLAS12 to reduce this contamination. A study of the efficiency is needed to evaluate the contamination.

The eH^+X missing mass to evaluate efficiency

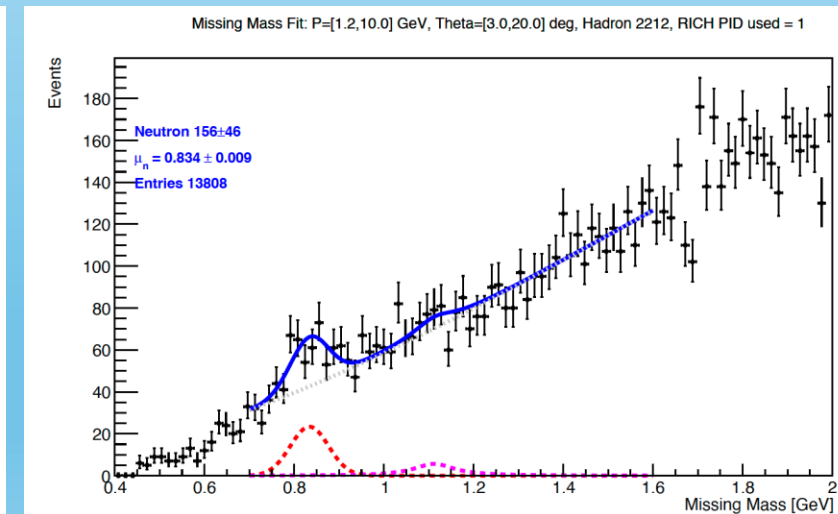
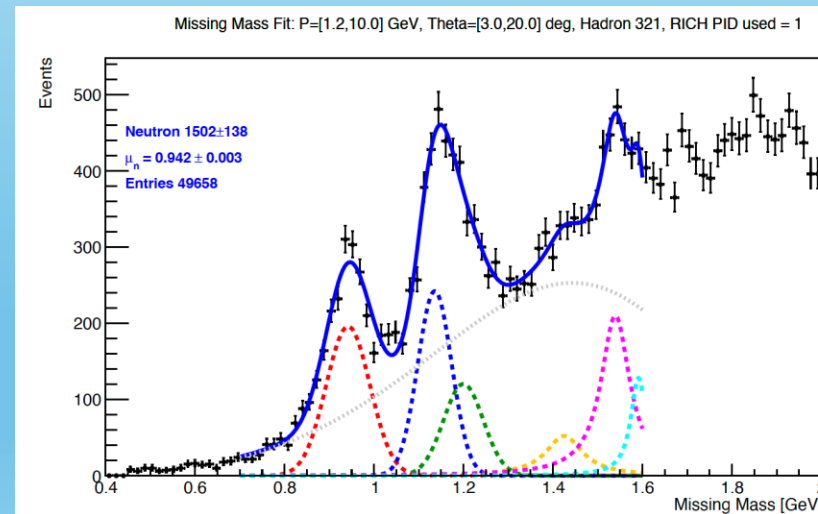
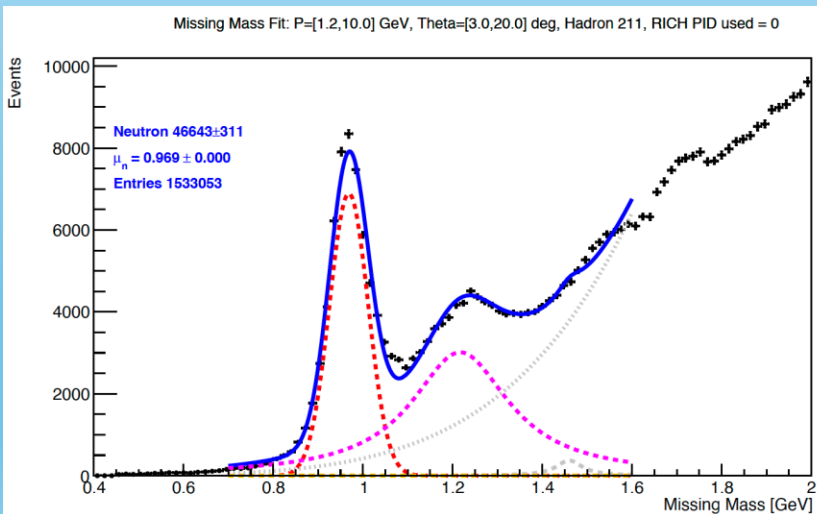
The plots show the missing mass for events including a positive hadron with momentum > 3 GeV, and both RICH PID and CLAS12 Event Builder PID (not including the RICH). No fiducial cut is applied.

- $e\pi^+n$ is an allowed exclusive process;
- eK^+n and epn are forbidden exclusive processes;



Fit of the missing mass

- The fitting curve: $f(mm) = \sum_i Gaussian(mm) + \sum_i BreitWigner(mm) + Bkg(mm)$
- Weibull function background: $Bkg(mm) = \frac{k}{\lambda} \left(\frac{mm}{\lambda}\right)^{k-1} e^{-\left(\frac{mm}{\lambda}\right)^k}$
- Other background tested: 2nd-degree polynomial, Chebyshev poly, crystal-ball, Argus function.



The identification probability

From the assumption that each neutron correspond to a real pion, I can define two quantities:

- The probability of identify a pion:

$$\eta_{\pi \rightarrow \pi} = \frac{\text{Number of exclusive neutrons in } e\pi^+X \text{ events}}{\text{Number of exclusive neutrons in } (e\pi^+X + eK^+X + epX) \text{ events}}$$

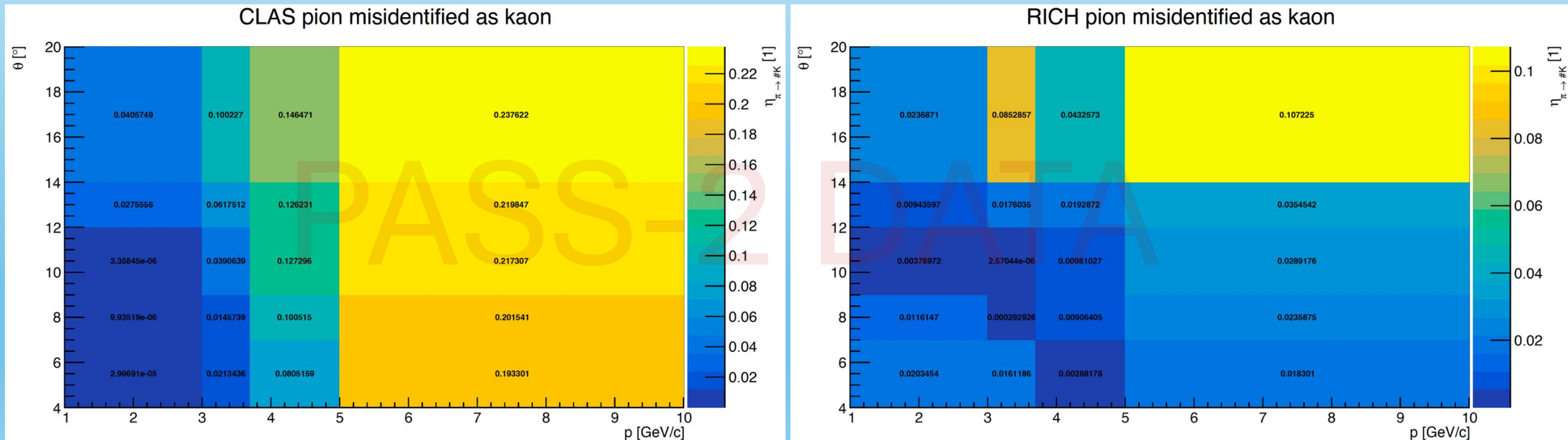
- The probability of misidentify a pion as a kaon:

$$\eta_{\pi \rightarrow K} = \frac{\text{Number of exclusive neutrons in } eK^+X \text{ events}}{\text{Number of exclusive neutrons in } (e\pi^+X + eK^+X + epX) \text{ events}}$$

$\eta_{\pi \rightarrow K} = \eta_{\pi \rightarrow K} (p_H, \theta_H)$ combined with the relative abundance of pion and kaon allows to determine the contamination of pion into the kaon sample.

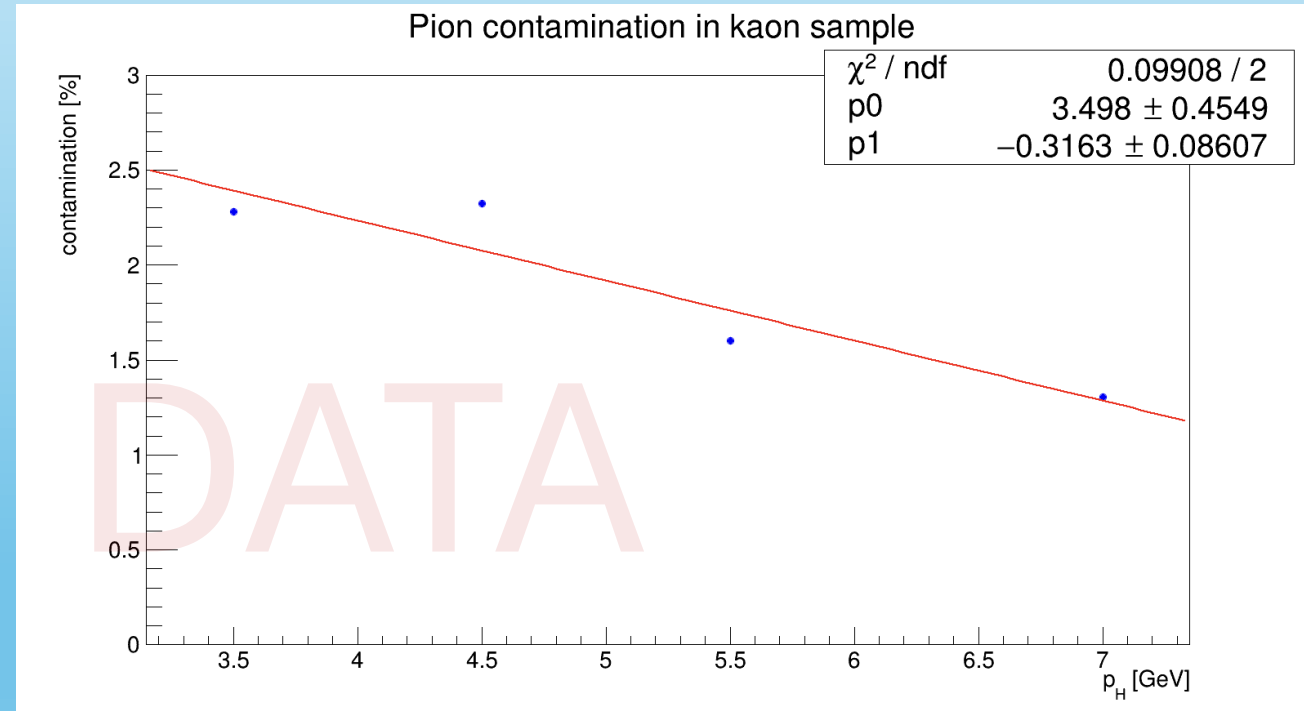
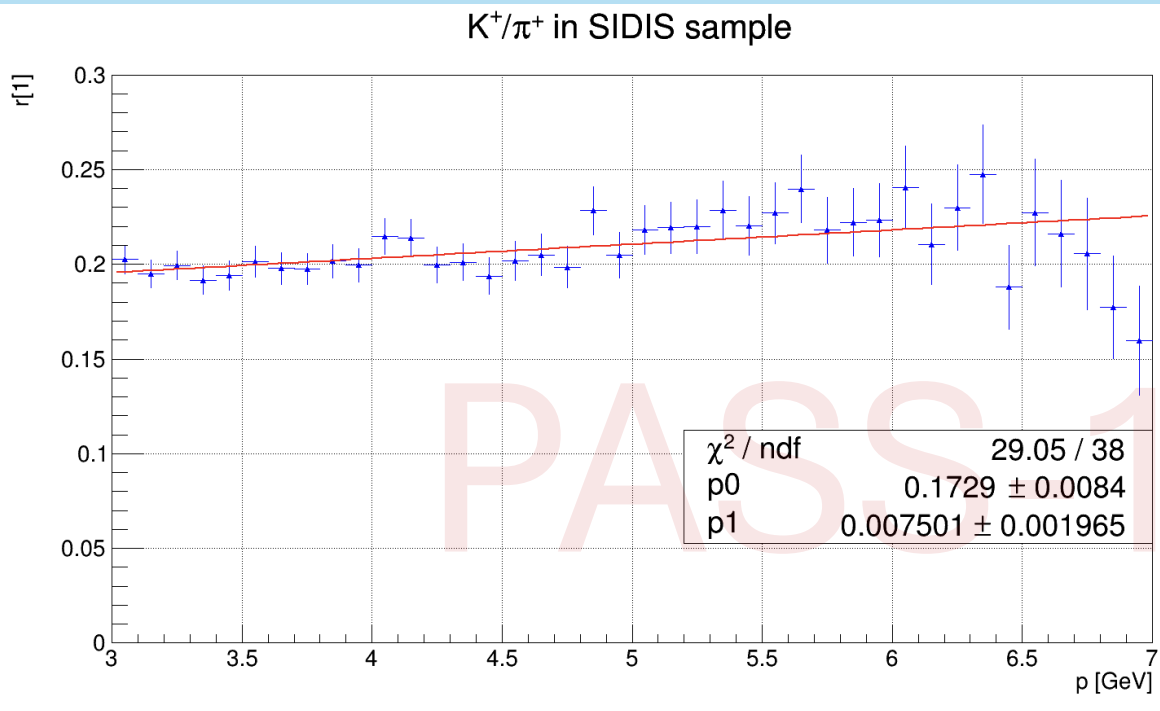
RICH efficiency

- Fraction of pion misidentified as kaon by RICH and CLAS12 PID (without RICH);
- Used pass-2 reconstruction (slightly worse than pass-1);
- The full alignment is almost complete and will extend the polar angle;
- It will allow to define a new fiducial cut based on the rich quality variables (RQ, RL).



The π contamination of K sample

- $\eta_{\pi \rightarrow K} = \eta_{\pi \rightarrow K}(p_H, \theta_H)$ combined with the relative abundance of pion and kaon allows to determine the contamination of pion into the kaon sample



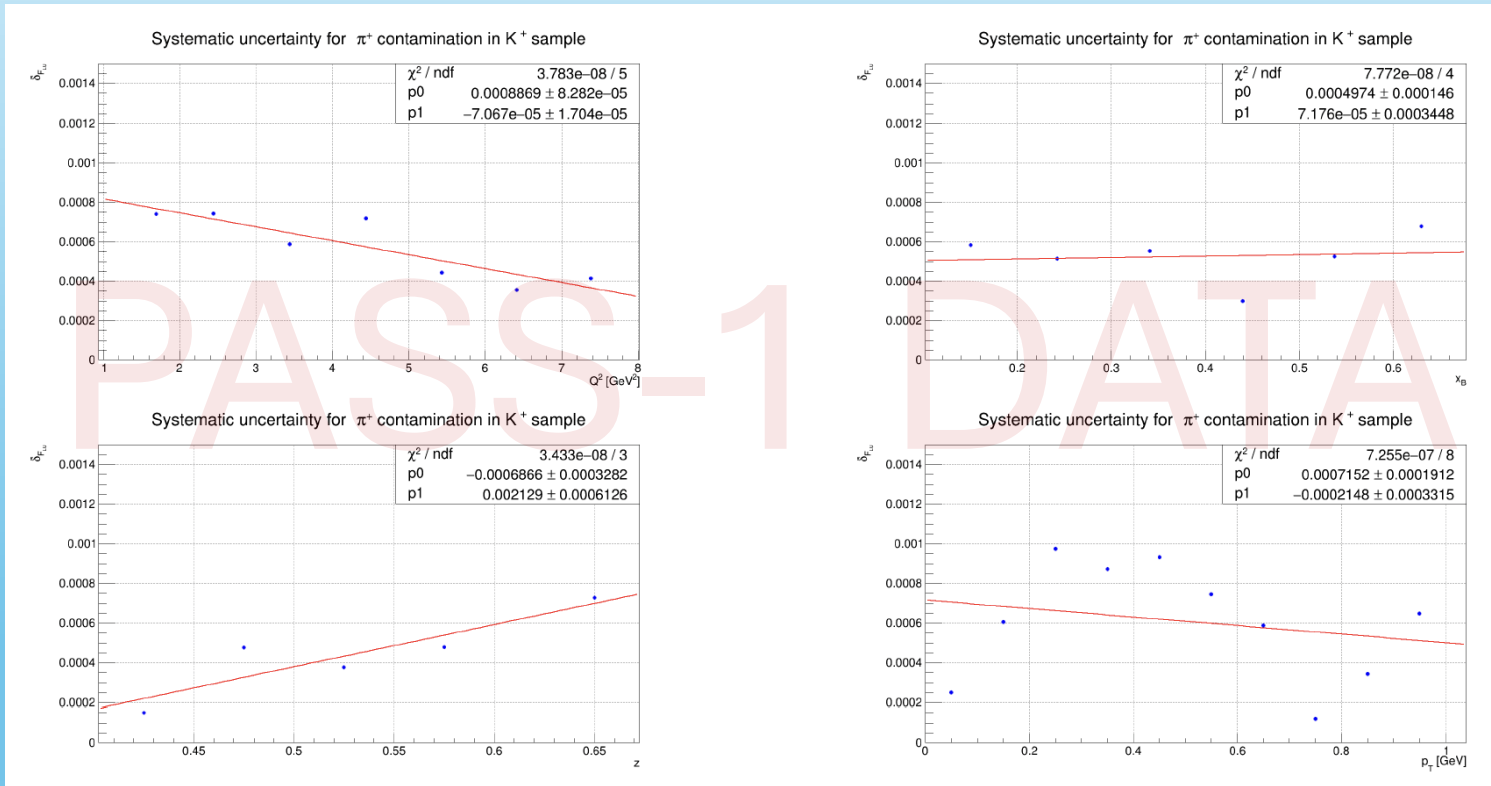
Systematic uncertainty due to π^+ contamination

$$F_{LU}^{meas} = F_{LU}^K + \delta F_{LU}^{cont} = F_{LU}^K + \left(\frac{N_\pi}{N_K} \Delta F_{LU} \right)$$

- N_π/N_K is the ratio between the number of pion contaminating and the kaon sample free of contamination.

- $\Delta F_{LU} = F_{LU}^K - F_{LU}^\pi$

- The pion structure function is obtained by applying the same analysis chain to the pion sample.



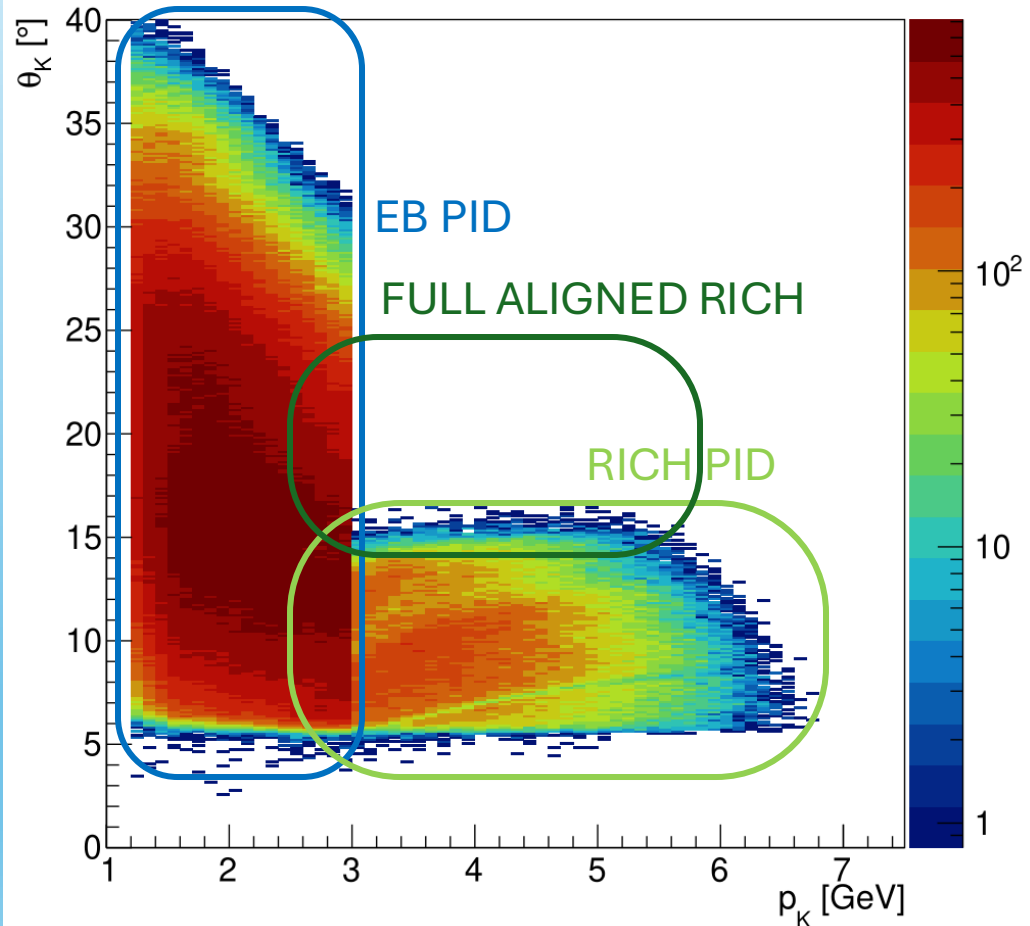
The study needs to be completed with polar angle dependence

Results with pass-1 alignment

Kaon phase space

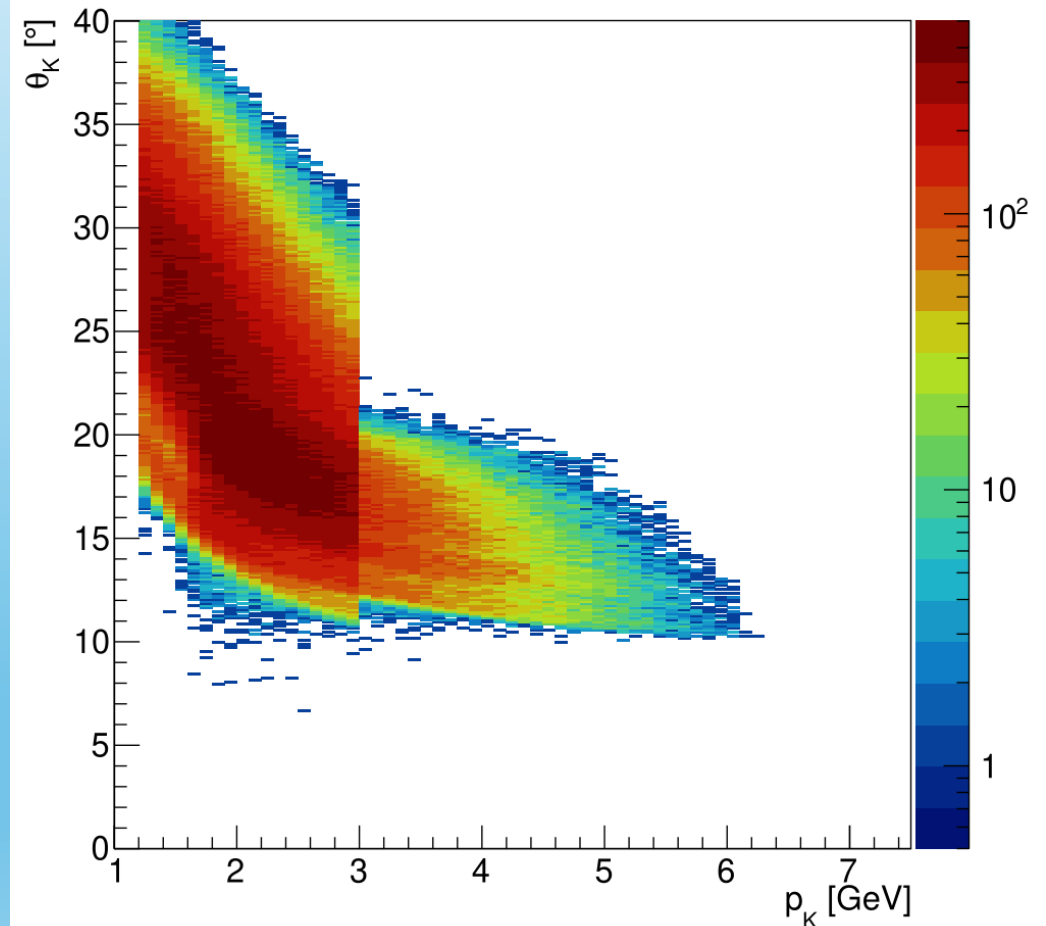
Inbending data

Hadron polar angle vs momentum



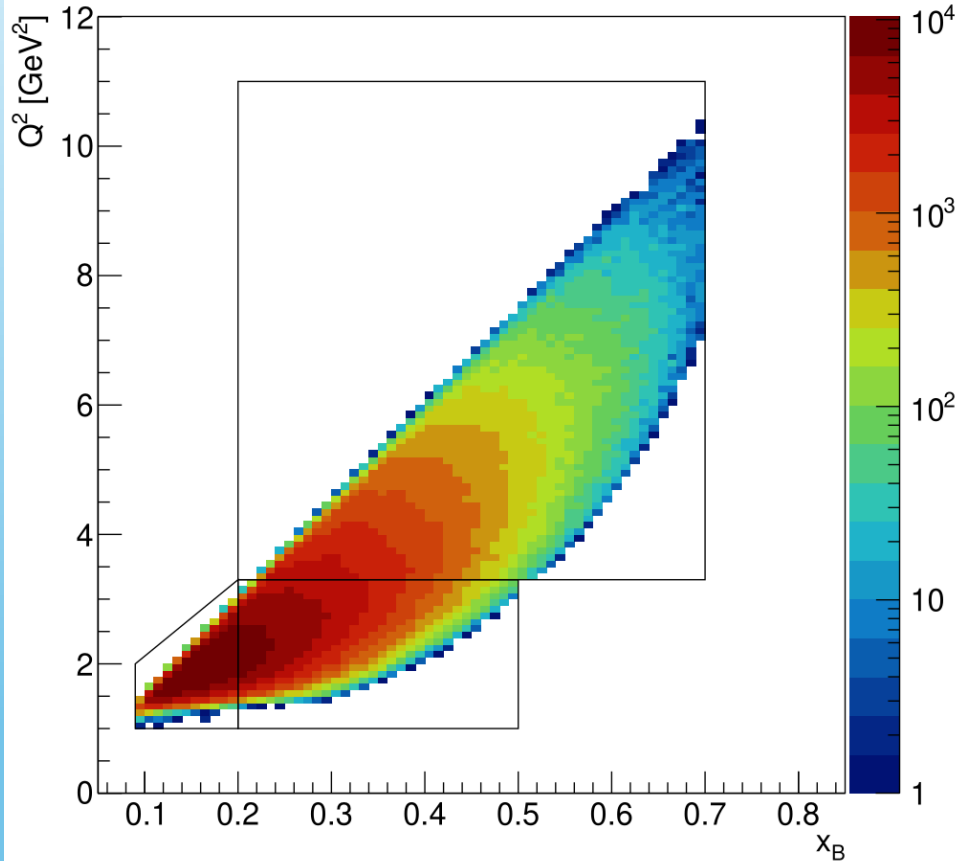
Outbending data

Hadron polar angle vs momentum

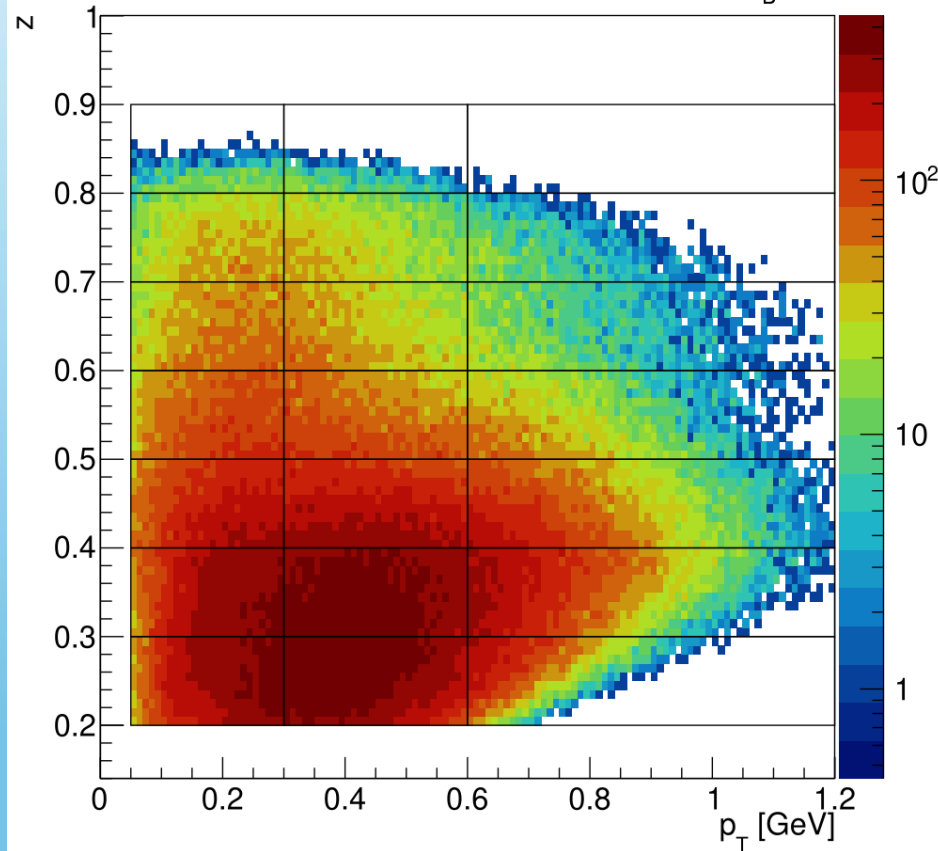


4-dimensional binning in Q^2 , x_B , z , p_T

Q^2 x_B distribution



z vs p_T distribution for bin $_{Q^2, x_B} 1$

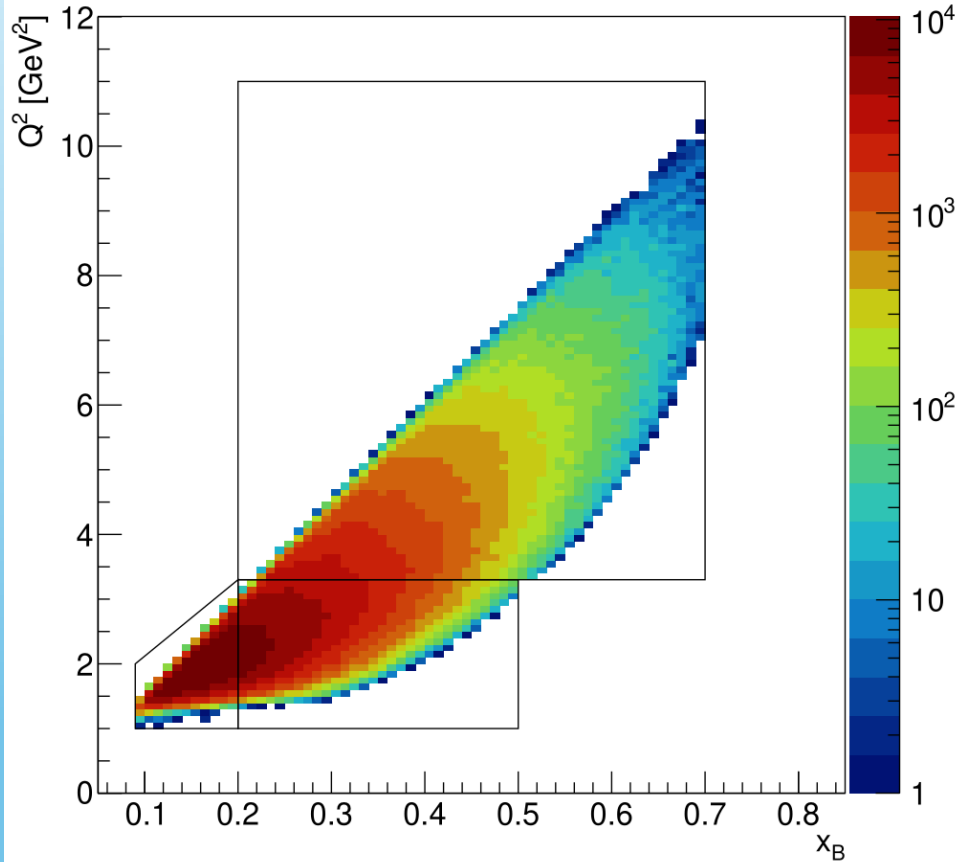


For each (Q^2, x_B) bin:

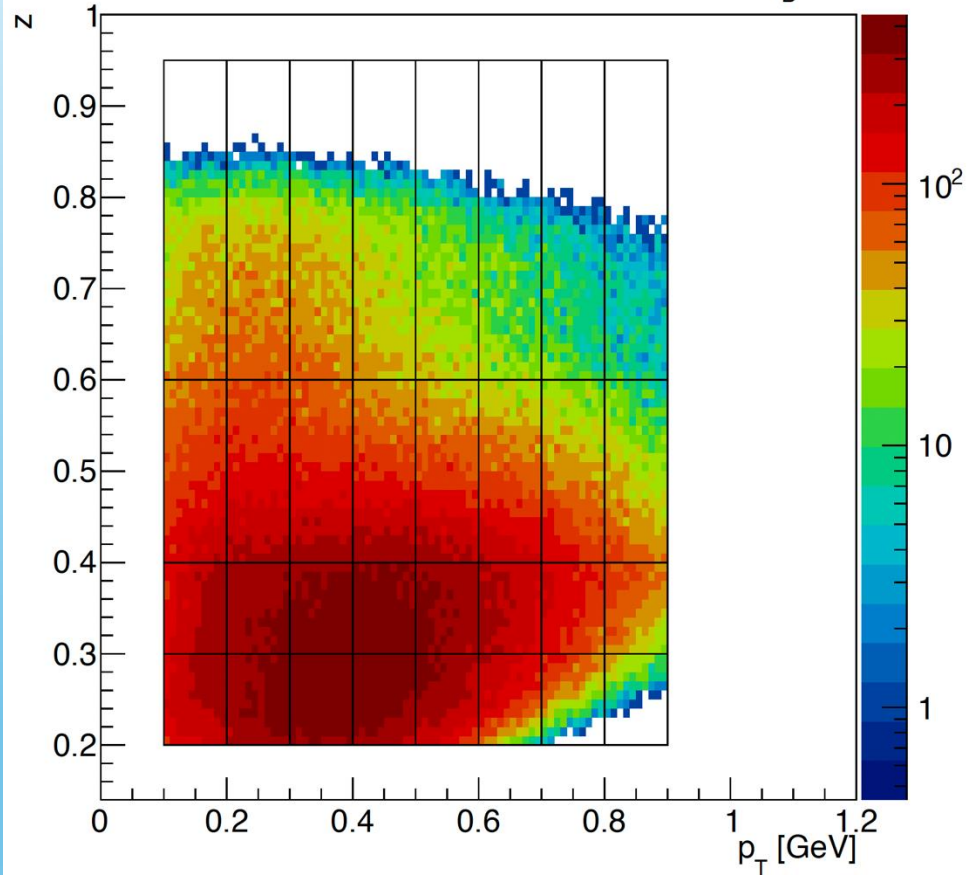
- **3 p_T bins** \rightarrow **BSA vs z**
- **4 z bins** \rightarrow **BSA vs p_T**

4-dimensional binning in Q^2 , x_B , z , p_T

Q^2 x_B distribution



z vs p_T distribution for bin $_{Q^2, x_B} 1$

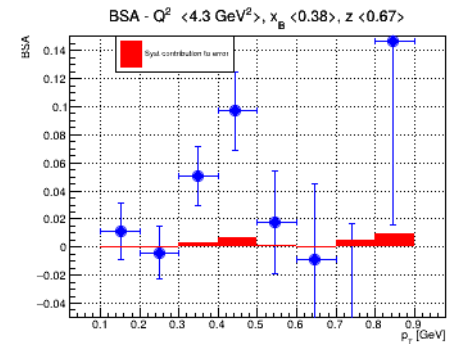
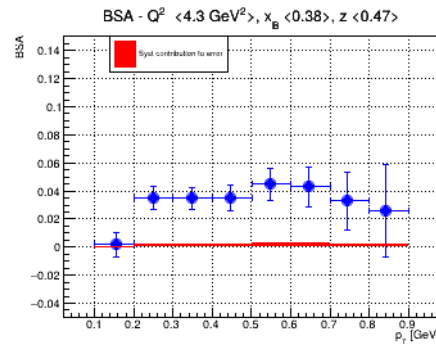
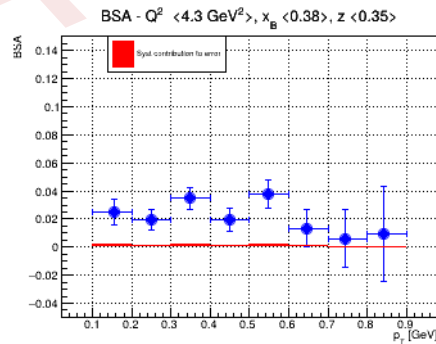
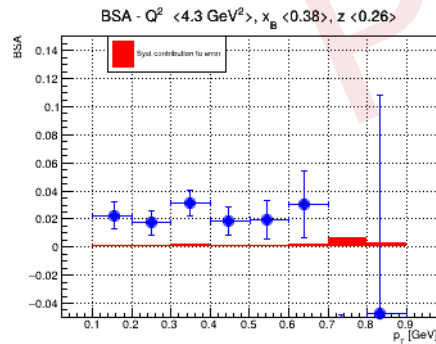
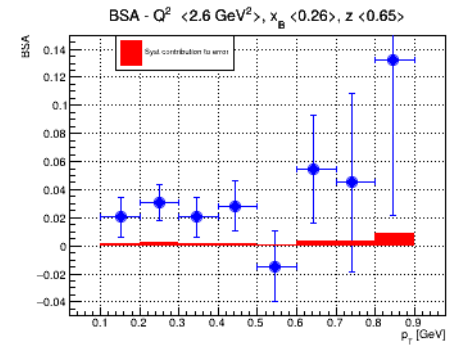
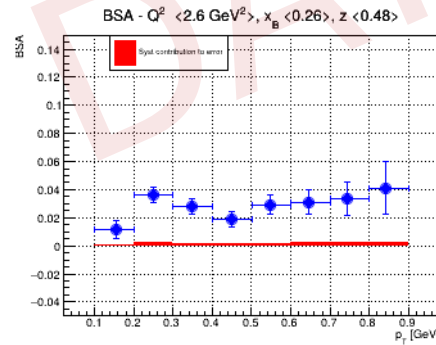
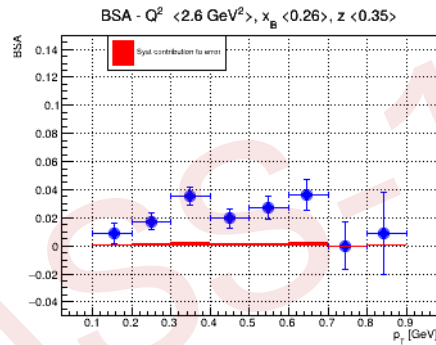
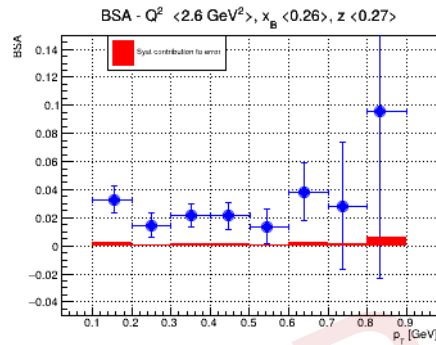
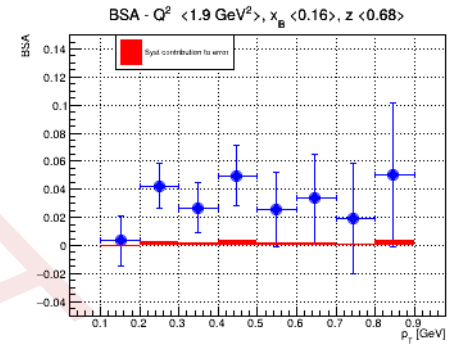
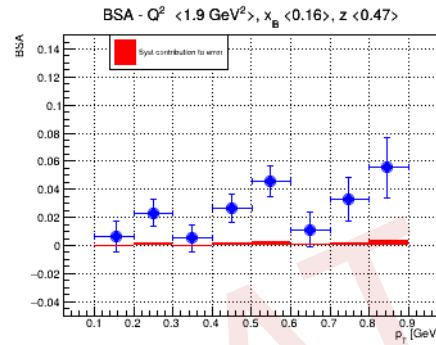
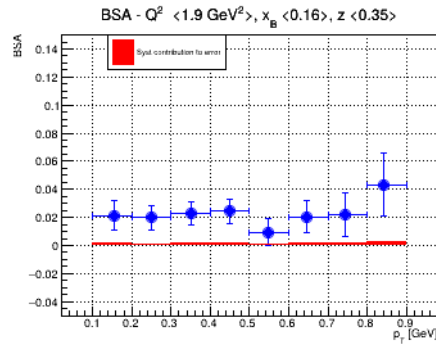
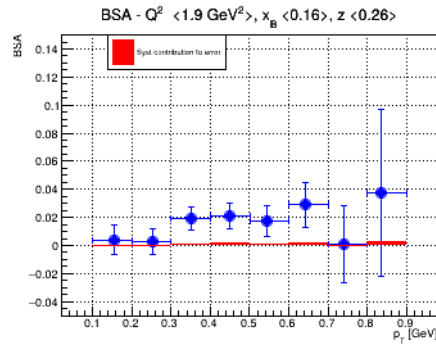


For each (Q^2, x_B) bin:

- 3 p_T bins \rightarrow BSA vs z
- **4 z bins \rightarrow BSA vs p_T**

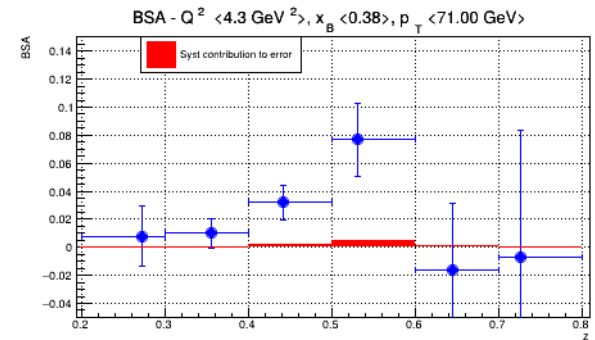
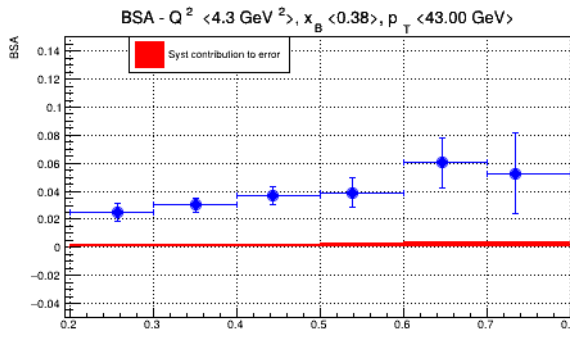
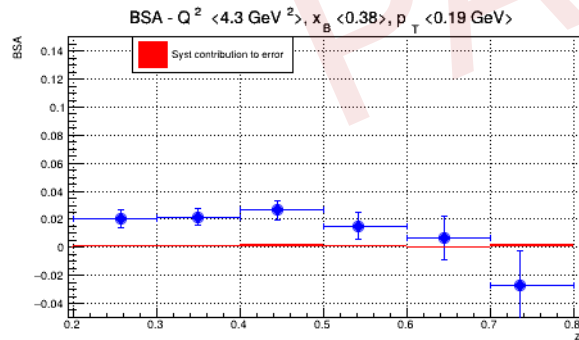
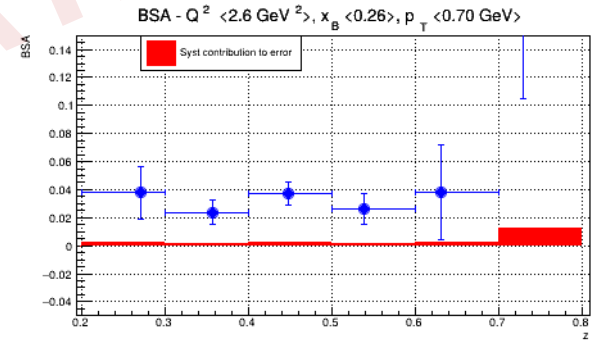
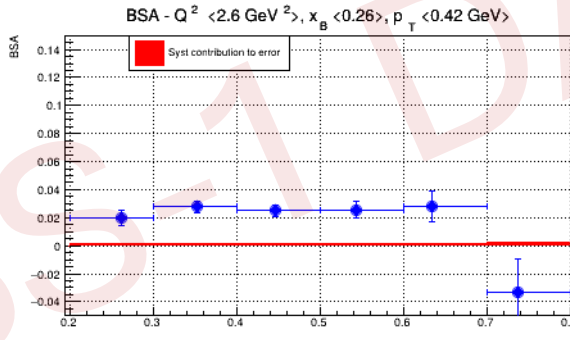
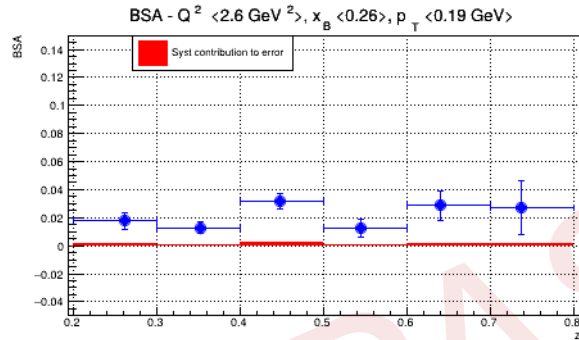
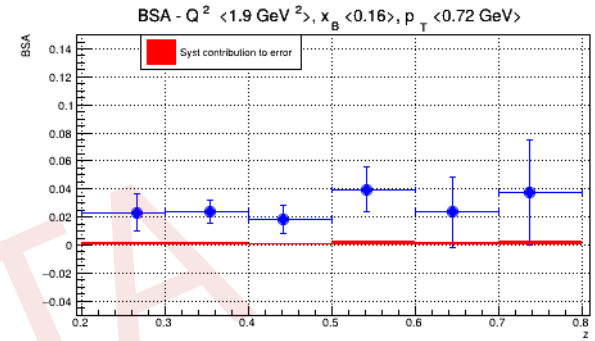
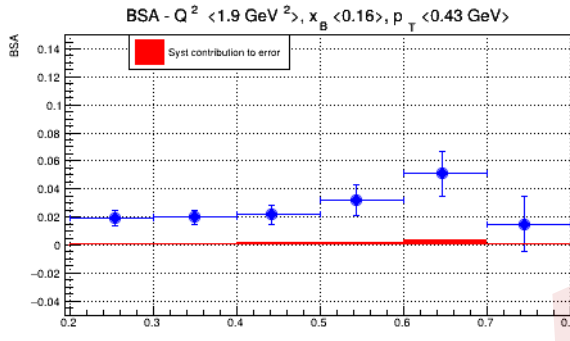
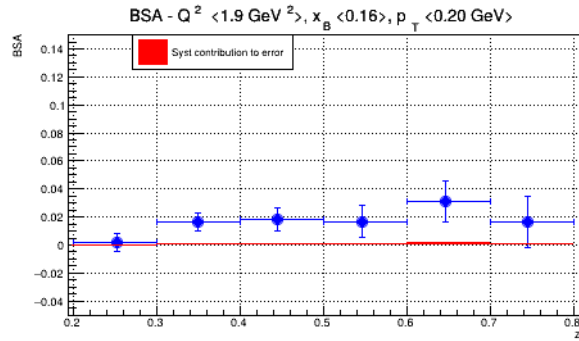
BSA as a function of p_T

Increasing Q^2, x_B

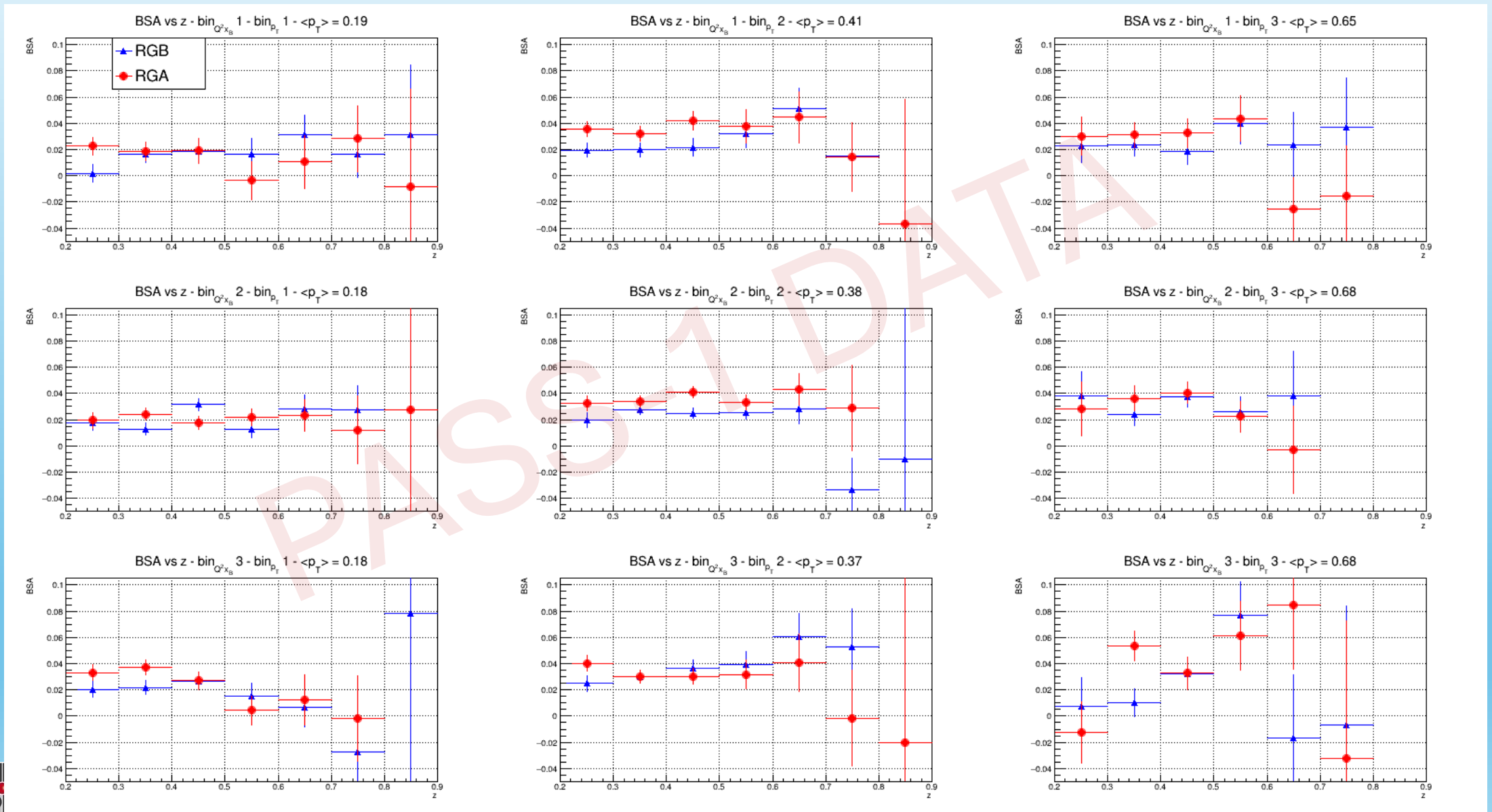


BSA as a function of z

Increasing Q^2, x_B



Comparison Hydrogen and Deuterium target



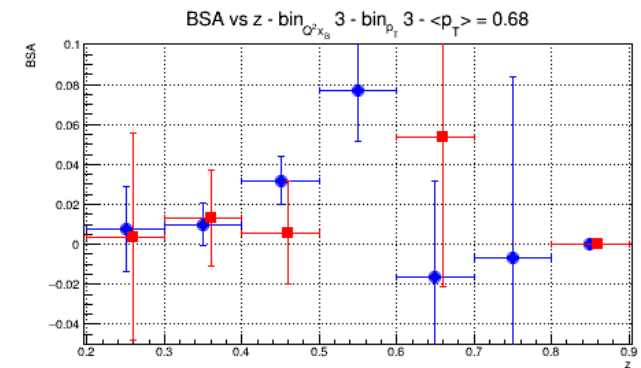
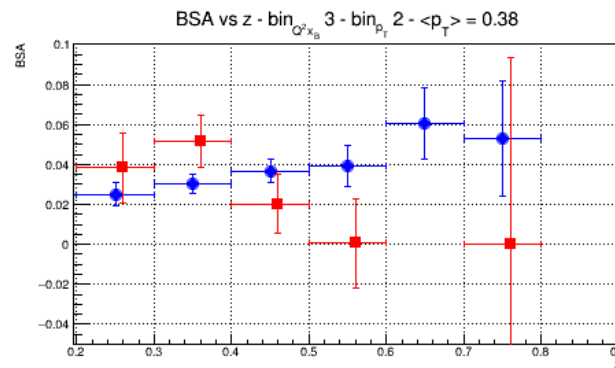
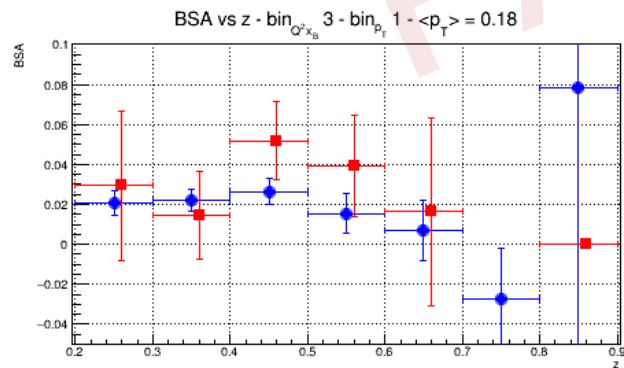
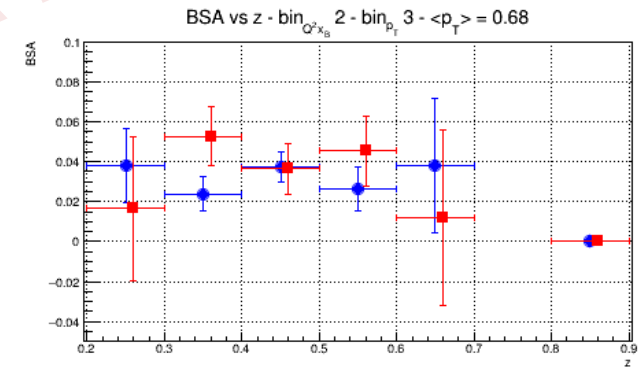
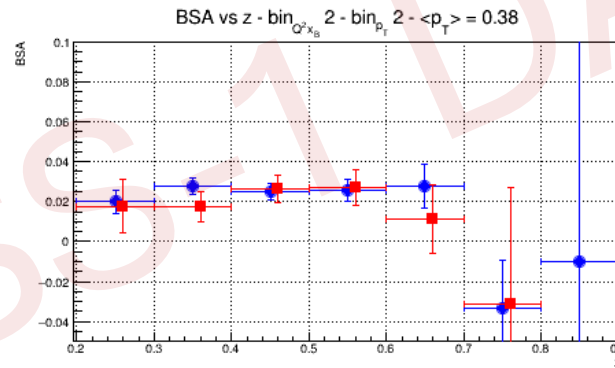
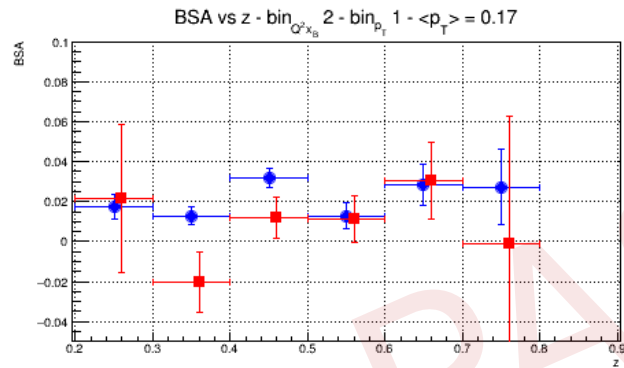
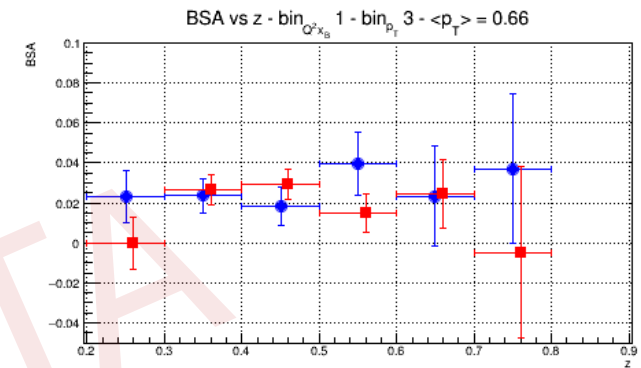
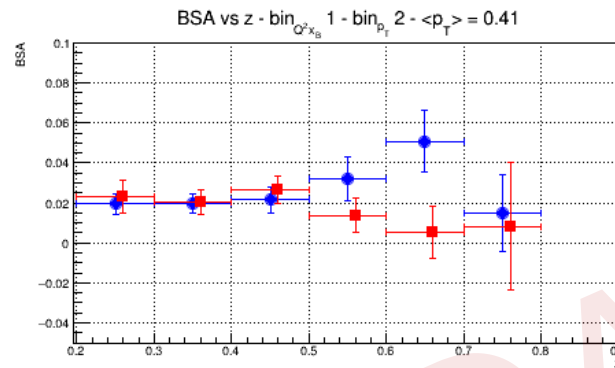
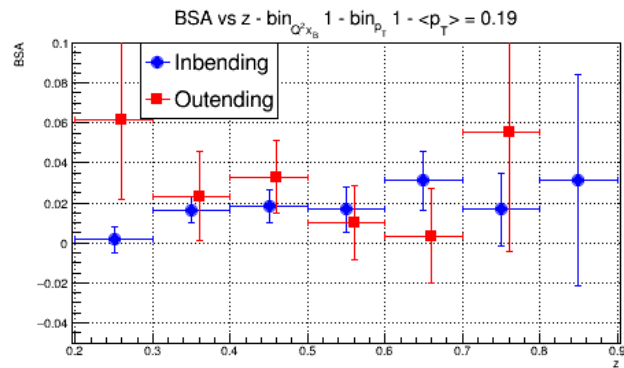
Conclusions

- CLAS12 at Jefferson Lab is a powerful tool to investigate TMD functions in the valence region;
- The RICH is a key detector to investigate SIDIS measurements with a clean kaon sample;
- The RICH alignment is nearly complete and extend the accessible phase space up to the largest polar angle available;
- The ongoing study of the RICH efficiency is essential for evaluating kaon sample contamination, which represents one of the main sources of systematic uncertainty for this measurement.
- Results obtained with pass-1 data show behavior consistent with theoretical expectations, namely:
 - Small BSA at low p_T ;
 - Weak dependance of the BSA on Z

Thank you

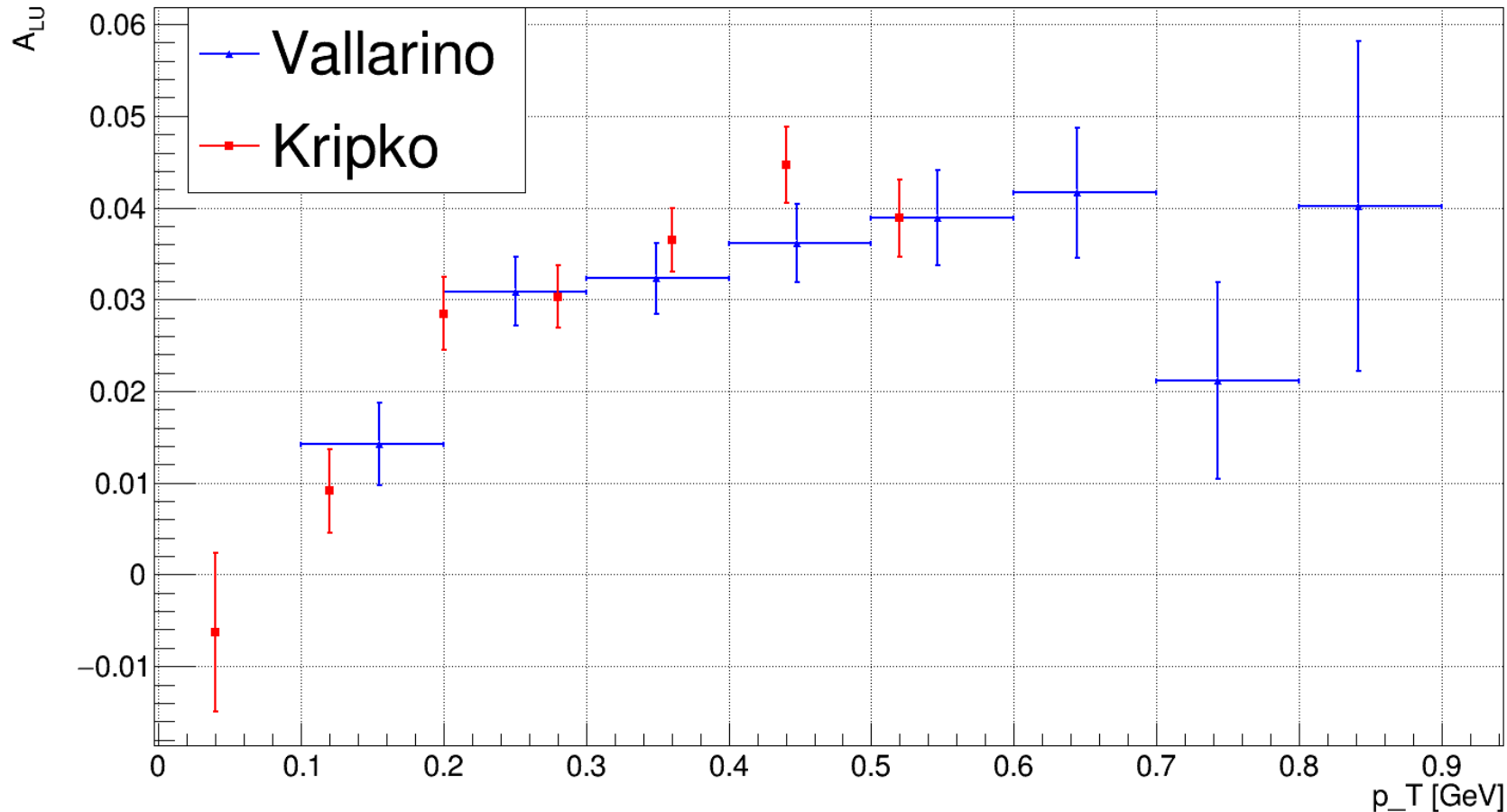
Backup slides

Comparison inbending – outbending dataset



Comparison with hydrogen target results

Comparison for $\langle z \rangle = 0.43$



- Comparison performed using inbending data;
- The results are comparable;
- Only statistical error is included